Contents lists available at ScienceDirect

Thin Solid Films

journal homepage: www.elsevier.com

In-situ X-ray photoelectron spectroscopy analysis of the initial growth of CdS thin films by chemical bath deposition

R. Garza-Hernández [a], A. Carrillo-Castillo [b], V.H. Martínez-Landeros [c], M.A. Martínez-Puente [a], E. Martínez-Guerra [a], F.S. Aguirre-Tostado [a, *]

[a] Centro de Investigación en Materiales Avanzados S. C. (Unidad Monterrey), Av. Alianza Norte 202, Parque PIIT, Apodaca CP 66628, Nuevo León, Mexico
[b] Instituto de Ingeniería y Tecnología, Universidad Autónoma de Ciudad Juárez, Av. del Charro 450, Ciudad Juárez CP 32310, Chihuahua, Mexico
[c] Facultad de Metalurgia, Universidad Autónoma de Coahuila, Carretera 57, km 5, Monclova C.P. 25720, Coahuila, Mexico

ARTICLE INFO

Keywords:
Cadmium sulfide
X-ray photoelectron spectroscopy
Chemical bath deposition
Nucleation

ABSTRACT

Cadmium sulfide is the main choice among n-type semiconductors for several solar cell technologies due to its excellent optical, structural and electronic characteristics. Even when it has been widely studied, there are still unsolved aspects related with the understanding of nucleation and growth mechanisms. For that, the initial growth stages of CdS deposited by chemical bath deposition (CBD) were carefully studied by in-situ X-ray photoelectron spectroscopy (XPS) by connecting a glove box with the CBD setup to the XPS introduction chamber. The CdS thin films were synthesized by CBD method onto glass substrates using $CdCl_2$ as the cadmium precursor, sodium citrate as the complexing agent and thiourea as the sulfur source. XPS analysis revealed the presence of $Cd(OH)_2$ and Cd-Citrate species, which facilitates nucleation to later promote the formation of CdS. During the deposition time (0–10 min) the pH changes from 12.1 to 10.8. Considering this, the following combination of mechanisms during the deposition: the hydroxide (above pH 11) and complex-decomposition (below pH 11) was proposed by using a distribution species diagram. The resulting films are close to the ideal stoichiometric CdS after 10 min of deposition. Furthermore, the film thicknesses determined by XPS ultra-thin film analysis, were about 2.37 and 13.7 nm, for 6 and 10 min, respectively, in good agreement with ellipsometry measurements.

1. Introduction

Cadmium sulfide is an n-type semiconductor with a direct wide band gap energy of 2.42 eV, high absorption coefficient ($>10^4\,cm^{-1}$) and mobility (0.1–10 cm^2/Vs) appropriated to be used as a window material for solar cells based on chalcogenide materials such as Cu(In, Ga)Se_2, CdTe, Cu_2ZnSnS_4, PbS [1–7]. Furthermore, CdS has shown great potential in the fabrication of electronic and photoelectronic devices, for example, thin film transistors [8,9] and photosensors [10]. CdS have been deposited by various methods such as chemical bath deposition (CBD) [5,11–13], evaporation [14], spray pyrolysis [15], sputtering [16], successive ionic layer adsorption and reaction [17], etc. However, CBD can produce CdS thin films with no cracks or pinholes, and excellent uniformity. Overall, CBD is a simple and inexpensive technique that allows to deposit several chalcogenides such as CdSe, ZnO, Sb_2S_3, Bi_2Se_3, ZnS, CuS, etc., through the variation of pH, salts concentrations and temperature [18]. CBD is an appropriate technique for device production at an industrial level due to the possibility of depositing at low temperature and large area semiconductors.

In recent years, extensive investigations on the optical, structural, chemical and electrical properties of bulk CdS deposited by CBD have been published [19–23]. However, there are remarkable few studies that focus on the experimental study and understanding the initial stages of nucleation and growth of CdS thin films. D.A Mazón Montijo et al. investigated the nucleation and growth of CdS thin films in an ammonia-free CBD process stating that the first nucleation centers are composed by $Cd(OH)_2$ as supported by X-ray photoelectron spectroscopy (XPS) results [24]. A. Oliva et al. studied the initial growth stages of CdS film deposition by CBD on different substrates such as glass, silicon and indium tin oxide. They studied the evolution of morphology and microstructure during the deposition of polycrystalline films, demonstrating by Auger electron spectroscopy

* Corresponding author.
Email address: servando.aguirre@cimav.edu.mx (F.S.-FAguirre-A Tostado)

https://doi.org/10.1016/j.tsf.2019.04.003
Received 19 December 2018; Received in revised form 16 March 2019; Accepted 1 April 2019
Available online xxx
0040-6090/

depth profiles that the CdS/substrate interface is not abrupt and the growth rate depends on the substrate [25]. Natalia S. Kozhevnikova et al. studied the initial growth of nanocrystalline CdS thin films using X-ray grazing incidence diffraction. The authors claimed that a buffer layer of cadmium hydroxide is formed between the silicon substrate and the cadmium sulfide thin film and is a key factor for the formation of adhesive CdS thin films [26]. The role of pH in chemical bath deposition is important because it defines the prevalent chemical species that will be present while the reaction is taking place [27]. Moreover, few authors mention the initial pH and its evolution along the reaction process which may have an effect in the film growth mechanism [28]. Even, when the vast majority of works use sodium citrate as the complexing agent, apparently no one considers the number of Cd-citrate ligands formed at different pH that can actively participate as promoters for the conversion of citrate-sulfide during the reaction in the same manner as hydroxide-sulfide does. The determination of species at different pH can help to elucidate the growth mechanism reaction. On the other hand, there are few works focused in detailed analysis of XPS.

However, despite the efforts to understand the nucleation and growth mechanism of CdS on glass using a suitable surface sensitive experimental technique, there are still unresolved questions like: Is the nucleation that gives rise to CdS more important in the solution than at the substrate surface? Is the reaction mechanism the same all across the deposition time? What is the deposition time required to get a stoichiometric CdS films?

In order to get information about the mentioned above, in this work we studied the chemistry of the surface semiconductor at the initial stages of CdS thin films by CBD growth on glass by carefully interrogating the surface chemistry with XPS. Additionally, the film thickness and S/Cd ratio at very early stages of growth were analyzed by XPS with the intention of investigating the deposition rate and chemistry. Finally, a growth mechanism supported by deposited film composition and the concentration of the Cd complex population in the solution at the working pH is discussed.

2. Experimental details

2.1. Materials

Cadmium chloride ($CdCl_2$, ≥ 99.99%) and thiourea (NH_2CSNH_2, 99.99%) from Sigma-Aldrich. Sodium citrate ($Na_3C_6H_5O_7{\cdot}2H_2O$, 99.3%) and potassium hydroxide (KOH, 85%) from Fermont and BDH Chemicals, respectively. Buffer solution (borate) pH 10 from J.T Baker.

2.2. Synthesis of CdS thin films

The deposition of cadmium sulfide thin films was carried out onto Corning glass substrates (2.5 cm × 7.5 cm × 0.1 cm). The glass substrates were ultrasonically cleaned in acetone, isopropyl alcohol and deionized water, and dried in flowing N_2. For the deposition of cadmium sulfide, 9 mL of 0.05 M $CdCl_2$ solution was poured into a 100 mL beaker. After that, 9 mL of 0.5 M sodium citrate, 3 mL of buffer solution pH 10, 3 mL of 0.5 M KOH, 4.5 mL of 0.5 M thiourea and 31.5 mL of deionized water were added with constant stirring [26]. Then the cleaned glass substrates were vertically immersed into the bath for the deposition to take place. The chemical reaction was carried out at 70 °C. The substrates with the deposited CdS film were removed from the beaker after 1, 3, 6 and 10 min and dried in N_2 flow. This procedure was performed in a glove box under N_2 atmosphere coupled to the introduction chamber of the XPS system with the purpose avoiding contamination by exposing the samples to the air (see Fig. 1).

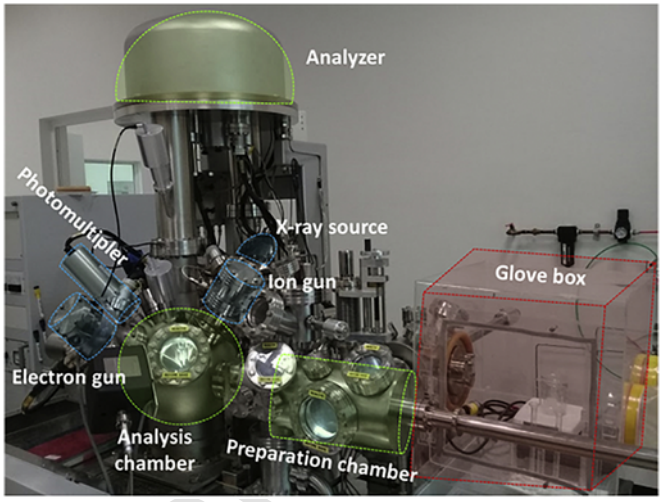

Fig. 1. Photograph of the ultra-high vacuum system used for in situ XPS measurements.

2.3. Instrumentation

Compositional and chemical states analyses on the films surface were carried out using X-ray photoelectron spectrometer Thermo Scientific Escalab 250 Xi. The photoelectrons were generated with a monochromatic Al Kα (1486.7 eV) X-ray source with a line width of 0.20 eV. The analysis chamber was kept at a base pressure of $< 4.3 \times 10^{-8}$ Pa. The photoelectrons were detected using a hemispherical analyzer with a pass energy of 20 eV. The relevant core levels C 1*s*, Si 2*p*, Cd 3*d*, S 2*p* and O 1*s* were considered to quantify the elemental atomic contents, using sensitivity factors from the instrument database. An electron flood gun was used to compensate the charging effect during the measurements. The electron beam energy and the emission current used were 2.0 V and 160.0 μA, respectively. Surface charging corrections to the shift in the binding energy were applied by fixing the energy of the C1*s* peak at 284.8 eV. The fitting procedure was an iterative process whereby all peaks were fitted using AAnalyzer® peak fitting software. The thickness was determined by XPS and corroborated by spectroscopic ellipsometry using a Horiba, Jobin Yvon UVISEL HR 320 ellipsometer at an incidence angle of 70° using photon energies in the range of 0.6 to 4.5 eV. The CdS concentration in the solution at different deposition times was obtained by quantifying the 516 nm absorption peak by using an UV-1800 UV–Vis Spectrophotometer from Shimadzu.

3. Results and discussion

Fig. 2 shows the high resolution spectra corresponding to the Cd 3*d*, S 2*p*, Si 2*p* and O 1*s* core levels of the films deposited at different time. The peaks centered at 405 and 411.9 eV are attributed to Cd $3d_{5/2}$ and Cd $3d_{3/2}$ orbitals and those located at 161.7 and 162.9 eV are correspond to S $2p_{3/2}$ and S $2p_{1/2}$ orbitals, respectively [29]. The Cd 3d and S 2p intensities show a drastic change between the films deposited at 3 and 6 min that can be attributed to the conclusion of the nucleation stage and the beginning of the growth stage.

The inset of Cd 3*d* region shows a magnification of the spectra for 1 and 3 min. From the deconvolution, there are clearly two Cd $3d_{5/2}$ peaks, component A at 405.04 eV corresponding to Cd-S and component B at 405.48 eV which is attributed to Cd-OH or Cd-Citrate [30]. The first main species adsorbed at the substrate are just Cd-OH or Cd-Citrate (predominant component B at 1 min of deposition) and S 2*p* signal is below the detection limit. After 3 min of deposition, there

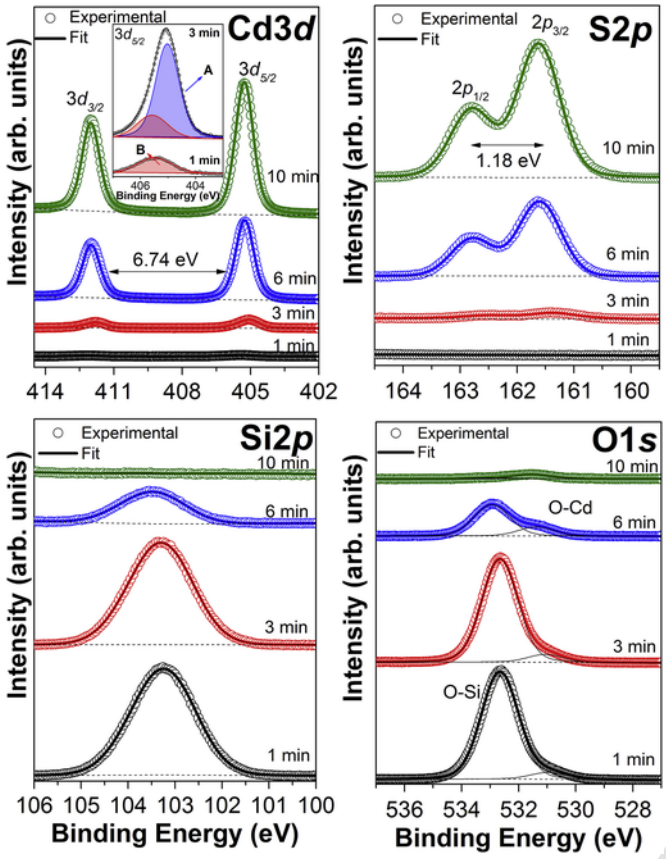

Fig. 2. XPS analysis of the Cd 3d, S 2p, Si 2p and O 1 s regions for CdS films deposited at 1, 3, 6 and 10 min by chemical bath deposition on glass substrates.

is a substantial increase of component A, while the components B remains unchanged. The relative intensity B/A is nearly zero making the peak B unnoticeable. The remarkable presence of the component A (Cd-S bonding) after 3 min would indicate that the anionic exchange for the conversion of $Cd(OH)_2$ and Cd-Citrate (CdL^-) in CdS has begun. The symmetry of the Cd-S peak for longer deposition times indicates the formation of a predominant CdS phase. The Si 2*p* spectra region shows a peak centered at 103.9 eV which is attributed to Si^{4+} chemically bonded to O (SiO_2) [31]. The O 1*s* spectra displays two peaks at 532.8 and 531.2 eV attributed to O—Si and O—Cd bonding, respectively [32,33]. Unsurprisingly, the intensity of Si 2*p* and O 1*s* corresponding to SiO_2 decreases while the CdS thickness increases. However, the O 1 s shoulder at 531.2 eV remains fairly constant at all times, which is consistent with the Cd-O (Cd-Citrate or $Cd(OH)_2$) component detected in the Cd 3*d* region. The areas and positions of main peaks are shown in Table 1.

Fig. 3a shows the peak area ratio of Cd 3*d* and S 2*p* with respect to the Si 2*p* from the SiO_2 substrate. The Cd/Si ratio is one order of magnitude larger than the S/Si ratio because of the photoionization cross section difference between the two core levels [34]. The relative atomic concentration is calculated from Eq. (1):

$$\%\text{Atomic concentration of Cd} = \frac{\frac{I_{Cd}}{ASF_{Cd}}}{\frac{I_{Cd}}{ASF_{Cd}} + \frac{I_S}{ASF_S}} * 100 \quad (1)$$

where I_X and ASF_X are the peak intensity and atomic sensitivity factor of element *X*, respectively. The calculation of surface composition by this method assumes that the film is homogenous within the volume analyzed by XPS. The stoichiometry ratio of the films deposited at 1, 3, 6 and 10 min are shown in Fig. 2b, in which can be seen that at 1 min the ratio is zero due to the lack of sulfur signal. During the incubation period (between 1 and 3 min), the chemical equilibria is reached and an initial nucleus of CdS is formed on the substrate surface. These CdS clusters are formed by the reaction of $Cd(OH)_2$ and Cd-Citrate with sulfide ions. The film formation takes place once the reaction to form the metal chalcogenide occurs. Moreover, after one minute, the stoichiometry ratio reached is higher than 0.5 (Fig. 3b), confirming that is necessary a minimum concentration of chalcogenide ions for the growth of the film. Afterwards, the film growth is favored, obtaining stoichiometry ratios in each deposition time until a [S/Cd] ratio of 0.92 at 10 min.

Fig. 4a shows the absorbance of solutions (black squares) and theirs respectively CdS concentrations (blue squares) obtained by UV–Vis spectroscopy. The CdS colloids in the solution are formed since the first minute, due to a perceptible change in absorbance. So, at this time, the nucleus of $Cd(OH)_2$ and Cd-Cit do not reach to diffuse to the substrate causing the anionic interchange in the solution, forming the CdS particles.

The film thickness (*d*) for ultra-thin films can be calculated by using the XPS signal of one of the elements on the film and one of the substrates. These is done by the following equation [35]:

$$\frac{I_{CdS}}{I_{SiO_2}} = \frac{I_{CdS^\infty}\left(1 - \exp^{(-d/\lambda_{CdS}\cos\theta)}\right)}{I_{SiO_2^\infty}\exp^{\left(-d/\lambda_{SiO_2}\cos\theta\right)}} \quad (2)$$

where λ_{CdS} and λ_{SiO2} are the attenuation lengths of photoelectrons emitted from the film and the substrate, respectively, [36] θ is the angle formed between the normal and the incident photon beam. I_{CdS} and I_{SiO2} are the peak intensities from CdS and SiO_2 and $I_{CdS,\infty}$ and $I_{SiO2,\infty}$ are the peak intensities from semi-infinite films of CdS and SiO_2 measured experimentally, respectively. The thickness in Eq. 2 can be calculated by using one of the XPS peak from the film, either from Cd or S. Fig. 3b shows the thickness as function of the deposition time while employing the Cd 3*d* (squares) or the S 2*p* intensity (circles). The CdS film thicknesses calculated from Eq. (2) either from the XPS intensity of the Cd 3d or S 2p peaks yields roughly the same values. The growth rate for the first 2 min is 0.1 nm/min and 3 nm/min afterward the minute 6 (Fig. 4b). The thicknesses obtained for 1, 3, 6 and 10 min were 0.03, 0.19, 3.20 and 15.68 nm, respectively. To validate this calculation, ellipsometry measurements were carried out for the films deposited at 6 and 10 min, obtaining thick-

Table 1
XPS Peak positions and areas for CdS thin films for several deposition times.

Samples	Binding energy (eV)				Areas (eV*cps)			
	$Cd3d_{5/2}$	$S2p_{3/2}$	Si2*p*	O1*s*	$Cd3d_{5/2}$	$S2p_{3/2}$	Si2*p*	O1*s*
1 min	405.5	–	103.1	532.6	7306	0	25,564	164,748
3 min	405.0	161.4	103.1	532.7	44,197	2116	24,377	156,725
6 min	405.2	161.6	103.4	532.9	329,631	17,606	7706	56,816
10 min	405.5	161.8	103.3	532.9	545,493	32,500	249	7905

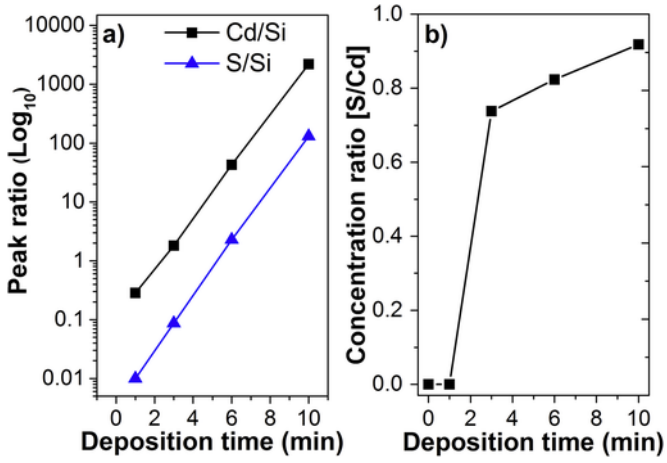

Fig. 3. a) Peak area ratio of Cd/Si (squares) and S/Si (triangles), and b) concentration ratio S/Cd ratio for CdS films deposited at 1, 3, 6 and 10 min by CBD.

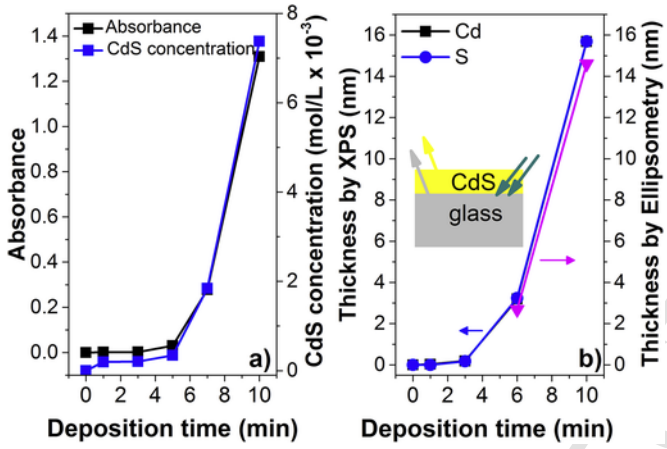

Fig. 4. a) Absorbance (black squares) and CdS concentration (blue squares) substrates and b) thickness of CdS films deposited for 1, 3, 6 and 10 min by CBD. (For interpretation of the references to colour in this figure legend, the reader is referred to the web version of this article.)

nesses of 2.67 ± 0.16 and 14.62 ± 0.77 nm. The thicknesses obtained by ellipsometry agree with those obtained by XPS. The reliability of the measurements could be ensured in the samples of 6 and 10 min of deposition due to the relative thick thicknesses and composition. As is discussed, the $Cd(OH)_2$ is deposited at 1 and 3 min, which has different optical properties compared with CdS making the fit procedure not reliable at this stage. After 6 min, CdS starts conferring to the thin film its respective optical properties. At this stage the CdS percentage regard to $Cd(OH)_2$ is high, therefore a good fit can be done in the 6 and 10 min samples. The models used in spectroscopic ellipsometry were validated through the obtained band gap energy values. The band gap energies for the 6 and 10 min samples were 2.44 eV and 2.31 eV, respectively, which correspond to the values reported in literature [26,29]. Therefore, CdS concentration and thickness plots exhibit the same exponential tendency, associating the increase of thickness do to the formation or precipitation in major extent of CdS in the solution.

The formation of a thin film could be explained by three different mechanisms such as ion by ion, hydroxide cluster and complex decomposition [37]. To determine, which is the most probable mechanism for the growth of CdS in this work, it is important to calculate the percentage of chemical species in the bath before adding the chalcogenide ion at different pH.

The mass balance of Cd considering all the complexes produced with the hydroxide and citrate (L) ions can be expressed by Eq (3).

$$\begin{aligned}[Cd_{total}] = {} & [Cd^{2+}] + [CdOH^{+}] + [Cd(OH)_2] \\ & + [Cd(OH)_3^{-}] + [Cd(OH)_4^{2-}] + [CdL^{-}] \\ & + [CdL_2^{4-}] + [CdHL] + [CdH_2L^{+}]\end{aligned} \tag{3}$$

Using the constant of formation (K) of each complex it was possible to determine the predominant species at the pH that the reaction takes place. The values of formation constants were taken from reported tables [38,39].

$$\begin{aligned}[Cd_{total}] = {} & [Cd^{2+}] \\ & + \left(1 + K_1[OH^{-}] + K_2[OH^{-}]^2 + K_3[OH^{-}]^3\right. \\ & + K_4[OH^{-}]^4 + K_5[L^{3-}] + K_6[L^{3-}]^2 \\ & \left. + K_7[L^{3-}][H^{+}] + K_8[L^{3-}][H^{+}]^2\right)\end{aligned} \tag{4}$$

Fig. 5a shows the percentage of species at several pH. The $Cd(OH)_2$ and CdL^{-} are the predominant species at pH 11. Furthermore, the free Cd^{2+} quantity in the medium remains low, which reduces its availability for the reaction, making easy to have control in the homogenous precipitation. Fig. 5b shows the variation of pH through the deposition time. The starting pH of the deposition is 12.1 and decrease with the time due to the precipitation of $Cd(OH)_2$ and the conversion to CdS. Taking in mind the species predominant calculated around this pH, the hydroxide mechanism dominates the initial steps of growth until seven minutes of deposition. Below pH 11 (deposition time larger) the predominant mechanism is complex-decomposition. The general mechanisms proposed is shown in Fig. 5c which is based in the interaction of the two- predominant species $Cd(OH)_2$ and CdL^{-} with the substrate depending of the deposition time as mentioned before. The oxygen atoms in the substrate will be bonded to positive Cd ions of Cd-containing negative complexes or Cd ions of $Cd(OH)_2$. The sulfide ions diffuse to surface, replacing the ligands and resulting in the formation of a CdS film.

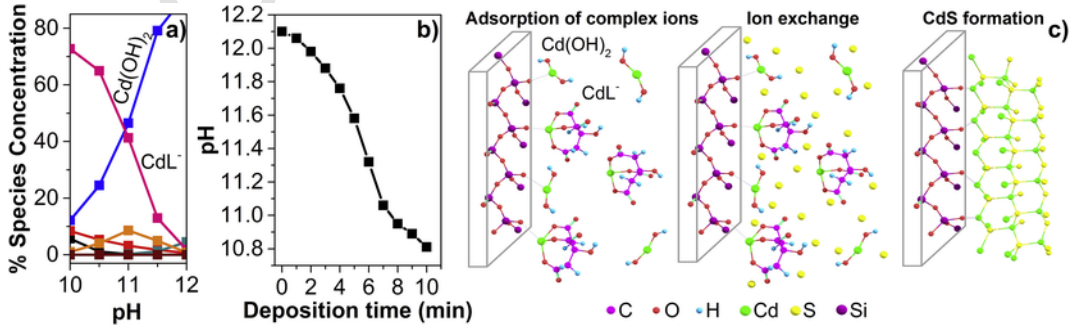

Fig. 5. a) Concentration of species in the chemical bath at pH 10–12. b) Experimental pH obtained at different deposition times. c) Schematic representation of mechanism for the formation of CdS film.

4. Conclusions

CdS thin films were deposited onto glass substrates using chemical bath deposition technique to estimate the chemical interaction of the reactants and compound stoichiometry at an initial growth stage. The thin films were prepared at different deposition times by using a constant temperature bath. The formation of CdS nucleus starts since the first minute in the solution but is perceived after 3 min in the substrate. The change in the thickness and stoichiometric ratio between 3 and 6 min of deposition is directly associated with the concentration of CdS in the solution. This change can be associated with the end of nucleation and the beginning of the CdS growth. After 10 min of deposition, a film close to the CdS stoichiometric ratio is reached. Thicknesses of the films ranging from 0.5 to 13.9 nm were estimated from XPS analysis. The growth mechanisms change across the deposition time: hydroxide until the first 6 min and then a complex-decomposition after this time, all based on the distribution species diagram. The reaction mechanism proposed is based in an anion exchange of hydroxide and citrate groups by sulfide ions suggested by XPS.

Acknowledgment

RGH want to thank to the Consejo Nacional de Ciencia y Tecnología (CONACyT)-México, for the granting of a scholarship. Also, authors thank to M.C. Gerardo Silva Vidaurri, Dra. Yolanda Peña Méndez, Dra. Leticia Torres Guerra and Dra. María Rocio Alfaro Cruz, for acquisition of XPS, UV–Vis and ellipsometry measurements, respectively.

References

[1] S. Rondiya, A. Rokade, B. Gabhale, S. Pandharkar, M. Chaudhari, A. Date, M. Chaudhary, H. Pathan, S. Jadkar, Effect of bath temperature on optical and morphology properties of CdS thin films grown by chemical bath deposition, Energy Procedia 110 (2017) 202–209, https://doi.org/10.1016/j.egypro.2017.03.128.

[2] Chen-ho Wu, H. Richard, Bube, thermoelectric and photothermoelectric effects in semiconductors: cadmium sulfide films, J. Appl. Phys. 45 (1974) 648–660, https://doi.org/10.1063/1.1663298.

[3] C. Min, M. Chuan-Ling, Z. De-Ming, T. Zi-Ao, A. Zheng-Hua, In-situ growth of a CdS window layer by vacuum thermal evaporation for CIGS thin film solar cell applications, Chin. Phys. B. 22 (2013) 107803–107806, https://doi.org/10.1088/1674-1056/22/10/107803.

[4] B. Liu, R. Luo, B. Li, J. Zhang, W. Li, L. Wu, L. Feng, J. Wu, Effects of deposition temperature and $CdCl_2$ annealing on the CdS thin films prepared by pulsed laser deposition, J. Alloys Compd. 654 (2016) 333–339, https://doi.org/10.1016/j.jallcom.2015.08.247.

[5] J.J. Scragg, P.J. Dale, L.M. Peter, G. Zoppi, I. Forbes, New routes to sustainable photovoltaics: evaluation of Cu_2ZnSnS_4 as an alternative absorber material, Phys. Status Solidi B 245 (2008) 1772–1778, https://doi.org/10.1002/pssb.200879539.

[6] A.S. Obaid, M.A. Mahdi, Z. Hassan, M. Bououdina, Preparation of chemically deposited thin films of CdS/PbS solar cell, Superlattice. Microst. 52 (2012) 816–823, https://doi.org/10.1016/j.spmi.2012.06.024.

[7] A.S. Obaid, Z. Hassan, M.A. Mahdi, M. Bououdina, Fabrication and characterizations of n-CdS/p-PbS heterojunction solar cells using microwave-assisted chemical bath deposition, Sol. Energy 89 (2013) 143–151, https://doi.org/10.1016/j.solener.2012.12.010.

[8] J.S. Meth, S.G. Zane, K.G. Sharp, S. Agrawal, Patterned thin film transistors incorporating chemical bath deposited cadmium sulfide as the active layer, Thin Solid Films 444 (2003) 227–234, https://doi.org/10.1016/S0040-6090(03)01053-8.

[9] G. Arreola-Jardón, L.A. González, L.A. García-Cerda, B. Gnade, M.A. Quevedo-López, R. Ramírez-Bon, Ammonia-free chemically deposited CdS films as active layers in thin film transistors, Thin Solid Films 519 (2010) 517–520, https://doi.org/10.1016/j.tsf.2010.08.097.

[10] S.R. Gosavi, C.P. Nikam, A.R. Shelke, A.M. Patil, S.-W. Ryu, J.S. Bhat, N.G. Deshpande, Chemical synthesis of porous web-structured CdS thin films for photosensor applications, Mater. Chem. Phys. 160 (2015) 244–250, https://doi.org/10.1016/j.matchemphys.2015.04.031.

[11] H. Zhang, X. Ma, D. Yang, Effects of complexing agent on CdS thin films prepared by chemical bath deposition, Mater. Lett. 58 (2003) 5–9, https://doi.org/10.1016/S0167-577X(03)00394-X.

[12] P. O'Brien, T. Saeed, Deposition and characterization of cadmium sulfide thin films by chemical bath deposition, J. Cryst. Growth 158 (1996) 497–504, https://doi.org/10.1016/0022-0248(95)00467-X.

[13] P. Roy, S.K. Srivastava, A new approach towards the growth of cadmium sulphide thin film by CBD method and its characterization, Mater. Chem. Phys. 95 (2006) 235–241, https://doi.org/10.1016/j.matchemphys.2005.06.010.

[14] L. Huang, Z.L. Wei, F.M. Zhang, X.S. Wu, Electronic and optical properties of CdS films deposited by evaporation, J. Alloys Compd. 648 (2015) 591–594, https://doi.org/10.1016/j.jallcom.2015.07.041.

[15] J. Hiie, T. Dedova, V. Valdna, K. Muska, Comparative study of nano-structured CdS thin films prepared by CBD and spray pyrolysis: annealing effect, Thin Solid Films 511–512 (2006) 443–447, https://doi.org/10.1016/j.tsf.2005.11.070.

[16] D. Kim, Y. Park, M. Kim, Y. Choi, Y.S. Park, J. Lee, Optical and structural properties of sputtered CdS films for thin film solar cell applications, Mater. Res. Bull. 69 (2015) 78–83, https://doi.org/10.1016/j.materresbull.2015.03.024.

[17] A. Mukherjee, B. Satpati, S.R. Bhattacharyya, R. Ghosh, P. Mitra, Synthesis of nanocrystalline CdS thin film by SILAR and their characterization, Phys. E. 65 (2015) 51–55, https://doi.org/10.1016/j.physe.2014.08.013.

[18] P.K. Nair, M.T.S. Nair, V.M. García, O.L. Arenas, Y. Peña, A. Castillo, I.T. Ayala, O. Gomezdaza, A. Sánchez, J. Campos, H. Hu, R. Suárez, M.E. Rincón, Semiconductor thin films by chemical bath deposition for solar energy related applications, Sol. Energy Mater. Sol. Cells 52 (1998) 313–344, https://doi.org/10.1016/S0927-0248(97)00237-7.

[19] Mouad Ouafi, Boujemaâ Jaber, Lahoucine Atourki, Najwa Zayyoun, Ahmed Ihlal, Ahmed Mzerd, Larbi Laânab, In situ low-temperature chemical bath deposition of CdS thin films without thickness limitation: structural and optical properties, Int. J. Photoenergy 1 (2018) 4549154–4549166, https://doi.org/10.1155/2018/4549154.

[20] N. Sathiya Priya, S. Shalini Packiam Kamala, V. Anbarasu, S. Anbuchudar Azhagan, R. Saravanakumar, Characterization of CdS thin films and nanoparticles by a simple chemical bath technique, Mater. Lett. 220 (2018) 161–164, https://doi.org/10.1016/j.matlet.2018.03.009.

[21] Nupur Saxenaa, Tania Kalsib, Prateek Uttamb, Pragati Kumar, Morphological evolution in nanocrystalline CdS thin films from flowers to salt rock like structures, Opt. Mater. 84 (2018) 625–630, https://doi.org/10.1016/j.optmat.2018.07.068.

[22] K.E. Nieto-Zepeda, A. Guillén-Cervantes, K. Rodríguez-Rosales, J. Santos-Cruz, D. Santos-Cruz, M. de la Olvera, O. Zelaya-Ángel, J. Santoyo-Salazar, L.A. Hernández-Hernández, G. Contreras-Puente, F. de Moure-Flores, Effect of the sulfur and fluorine concentration on physical properties of CdS films grown by chemical bath deposition, Results Phys. 7 (2017) 1971–1975, https://doi.org/10.1016/j.rinp.2017.06.008.

[23] A. Slonopas, H. Ryan, B. Foley, Z. Sun, K. Sun, T. Globus, P. Norris, Growth mechanisms and their effects on the opto-electrical properties of CdS thin films prepared by chemical bath deposition, Mater. Sci. Semicond. Process. 52 (2016) 24–31, https://doi.org/10.1016/j.mssp.2016.05.011.

[24] D.A. Mazón-Montijo, M. Sotelo-Lerma, M. Quevedo-López, M. El-Bouanani, H.N. Alshareef, F.J. Espinoza-Beltrán, R. Ramírez-Bon, Morphological and chemical study of the initial growth of CdS thin films deposited using an ammonia-free chemical process, Appl. Surf. Sci. 254 (2007) 499–505, https://doi.org/10.1016/j.apsusc.2007.06.041.

[25] A.I. Oliva, R.C. Rodríguez, O. Ceh, P.B. Pérez, F.C. Briones, V. Sosa, First stages of growth of CdS films on different substrates, Appl. Surf. Sci. 148 (1999) 42–49, https://doi.org/10.1016/S0169-4332(99)00136-1.

[26] N.S. Kozhevnikova, A.A. Rempel, F. Hergert, A. Magerl, Structural study of the initial growth of nanocrystalline CdS thin films in a chemical bath, Thin Solid Films 517 (2009) 2586–2589, https://doi.org/10.1016/j.tsf.2008.10.014.

[27] Paul O'Brien, John McAleese, Developing an understanding of the processes controlling the chemical bath deposition of ZnS and CdS, J. Mater. Chem. 8 (11) (1998) 2309–2314, https://doi.org/10.1039/A804692A.

[28] Y. Hashimoto, N. Kohara, T. Negami, N. Nishitani, T. Wada, Chemical bath deposition of Cds buffer layer for CIGS solar cells, Sol. Energy Mater. Sol. Cells 50 (1998) 71–77, https://doi.org/10.1016/S0927-0248(97)00124-4.

[29] V.G. Bhidet, S. Salkalachent, A.C. Rastogit, C.N. Raot, M.S. Hegdet, Depth profile composition studies of thin film $CdS:Cu_2S$ solar cells using XPS and AES, J. Phys. D: Appl. Phys. 14 (1981) 11647–11656, https://doi.org/10.1088/0022-3727/14/9/012.

[30] D.E. Zhang, X.D. Pan, H. Zhu, S.Z. Li, G.Y. Xu, X.B. Zhang, A.L. Ying, Z.W. Tong, A simple method to synthesize cadmium hydroxide nanobelts, Nanoscale Res. Lett. 3 (2008) 284–288, https://doi.org/10.1007/s11671-008-9150-4.

[31] Takeo Hattori, Tatsushi Nishina, Studies of SiO_2 and Si/SiO_2 interfaces by XPS, Surf. Sci. 86 (1979) 555–561, https://doi.org/10.1016/0039-6028(79)90434-5.

[32] M.L. Miller, R.W. Linton, X-ray photoelectron spectroscopy of thermally treated silica (SiO_2) surfaces, Anal. Chem. 57 (12) (1985) 2314–2319, https://doi.org/10.1021/ac00289a033.

[33] J.S. Hammondz, S.W. Gaarenstroom, Nicholas Winograd, X-ray photoelectron spectroscopic studies of cadmium- and silver-oxygen surfaces, Anal. Chem. 47 (1975) 2193–2199, https://doi.org/10.1021/ac60363a019.

[34] J.J. Yeh, I. Lindau, Atomic subshell photoionization cross sections and asymmetry parameters: $1 < Z < 103$, At. Data Nucl. Data Tables 32 (1985) 1, https://doi.org/10.1016/0092-640X(85)90016-6.

[35] R. Vitchev, J. Pireaux, T. Conard, H. Bender, J. Wolstenholme, C. Defranoux, X-ray photoelectron spectroscopy characterisation of high-k dielectric Al_2O_3 and HfO_2 layers deposited on SiO_2/Si surface, Appl. Surf. Sci. 235 (2004) 21–25, https://doi.org/10.1016/j.apsusc.2004.05.135.

[36] C. J. Powell, and A. Jablonski, NIST Standard Reference Database 82 "NIST Electron Effective-Attenuation-LengthDatabase", 10.18434/T4MK5P.
[37] G. Hodes, Chemical Solution Deposition of Semiconductor Films, Marcel Dekker Inc., New York, US, 2002.
[38] J.G. Speight, Lange's Handbook of Chemistry, Mc. Graw- Hill Education, New York, US, 2005.
[39] A.E. Martell, R.M. Smith, Critical Stability Constants, Springer Science Business Media, New York, US, 1982.